Available online at www.sciencedirect.com
ScienceDirect
Journal of Power Sources 170 (2007) 433–440
JOURNAL OF POWER SOURCES
www.elsevier.com/locate/jpowsour

Crystal chemistry modification of lithium nickel cobalt oxide cathodes for lithium ion rechargeable batteries

S. Sivaprakash [a], S.B. Majumder [a,*], S. Nieto [b], R.S. Katiyar [c]

[a] *Materials Science Centre, Indian Institute of Technology, Kharagpur 721302, India*
[b] *School of Science and Technology, University of Turabo, Gurabo, PR 00778-3030, USA*
[c] *Department of Physics, University of Puerto Rico, San Juan, PR 00931, USA*

Received 26 February 2007; received in revised form 12 April 2007; accepted 13 April 2007
Available online 22 April 2007

Abstract

As a cathode material for lithium ion rechargeable batteries, $LiNi_{0.8}Co_{0.2}O_2$ (LNCO) is one of the most attractive candidates for high power electronic devices. In the present work, we have synthesized LNCO powder by solid-state route. The discharge capacity and the capacity retention of LNCO cathode are found to be ~100 mAh g^{-1} and ~63%, respectively. Molybdenum doping, replacing parts of cobalt ion in LNCO lattice increases the discharge capacity (~157 mAh g^{-1}) and improve its capacity retention characteristics. Through X-ray Rietveld analyses, we have found that Mo doping increases the inter-slab spacing between the (Co,Ni)O_2 octahedral layers which provides easier Li^{1+} intercalation leading to improved electrochemical properties in the modified cathode.

Keywords: Li ion batteries; Cathode materials; Electrochemical properties; Solid-state synthesis and Rietveld refinement

1. Introduction

Commercial lithium ion batteries utilize lithium cobalt oxide ($LiCoO_2$) as cathode material. The capacity of $LiCoO_2$ cathode (~140 mAh g^{-1}) is low as Li^+ extraction beyond 0.5 M is not structurally permitted. Due to its higher discharge capacity (~200 mAh g^{-1}), lithium nickel oxide [$LiNiO_2$ (LNO)] has been considered as an effective alternate to lithium cobalt oxide cathodes. However, before the commercial acceptance of lithium nickel oxide as cathode material, several material related shortcomings need to be solved. These problems and related research issues are summarized as follows [1–4]: (i) the cation disorder of Ni ions in the lithium site lead to a lithium deficient pristine material with the stoichiometry $(Li_{1-z}Ni_z^{2+})(Ni_z^{2+}Ni_{1-z}^{3+})O_2$. During the electrochemical charging Ni^{2+} in the Li plane oxidized to Ni^{3+} state and the resulting structural distortion inhibits Li ion intercalation during first discharge resulting a huge polarization loss. Therefore, reduction of Ni^{3+} to Ni^{2+} during the cathode synthesis and the migration of Ni^{2+} ions in the Li^{1+} site need to be inhibited. (ii) Ni^{3+} (d^7) in its low spin $t^6{}_{2g}e^1{}_g$ configuration is prone to Jahn–Teller distortion and as a result the NiO_6 octahedra are locally distorted and the induced strain leads to the discontinuity to the particle–particle/particle–electrode contact, which eventually increases the electrode resistance and capacity fading. The capacity fading should be minimized by reducing the Jahn–Teller distortion. (iii) In its charged state, $Li_{1-x}NiO_2$ loses oxygen through an exothermic reaction. The rise in temperature is alarming especially when organic liquid electrolyte is used and its flash point is reached resulting a cell explosion. Additionally, with moderate rise in temperature the migration of divalent Ni ion is expedited from octahedral 3b site to 3a Li plane. Attempts should therefore be made to increase the thermal stability of lithium nickel oxide. (iv) Even when the pristine LNO is stoichiometric, during repeated cycling its layered rhombohedral structure is reported to be partially transformed into an electrochemically inactive spinel structure. The structural transformation with repeated cycling leads to capacity fading due to the loss of intercalating Li contents of the pristine material. In order to improve the capacity retention, therefore, the layered rhombohedral to spinel transformation should be inhibited.

It remains a major challenge to synthesize phase pure LNO without the Ni and Li cationic disorder. Although materials such

* Corresponding author. Tel.: +91 3222 283986; fax: +91 3222 255303.
E-mail address: subhasish@matsc.iitkgp.ernet.in (S.B. Majumder).

0378-7753/$ – see front matter © 2007 Elsevier B.V. All rights reserved.
doi:10.1016/j.jpowsour.2007.04.029

as LNO and lithium manganese oxide [$LiMnO_2$ (LMO)] are isostructural with $NaFeO_2$ type $LiCoO_2$, the problem of Ni and Mn ion migration is severe in LNO and LMO even at ~50 °C and room temperature, respectively, while on the other hand the Co ion hardly migrates to Li plane even at higher temperature. A plausible explanation has been reported in literature by calculating the crystal field stabilization energies (CFSE) of Mn^{3+}, Ni^{3+} and Co^{3+} cations in octahedral and tetrahedral sites. For the low spin configurations of Ni^{3+} ($3d^7$), Co^{3+} ($3d^6$) and high spin configuration of Mn^{3+} ($3d^4$) in octahedral coordination, the octahedral site stabilization energy (OSSE) (the difference between the crystal field stabilization energy between the CFSE values of octahedral and tetrahedral coordination) increases in the order of Mn^{3+} (−4.22 Dq) < Ni^{3+} (−12.67 Dq) < Co^{3+} (−21.33 Dq) [5]. A larger OSSE value for Co^{3+} ions makes the migration of Co ions difficult, whereas a comparatively lower OSSE for Ni and Mn ions make such migration kinetically favorable at slightly elevated and room temperature, respectively.

To stabilize the layered hexagonal structure of $LiNiO_2$, therefore we have substituted part of Ni^{3+} with Co^{3+} to synthesize $LiNi_{0.80}Co_{0.20}O_2$ by solid-state route. Several recent research reports have indicated that during charging, Ni^{3+} is oxidized to Ni^{4+} state (whereas the valence state of Co^{3+} remains invariant) and electrode material becomes unstable in the oxidized state [1,4,6]. To impart better stability of the de-intercalated cathode we have also synthesized Mo^{6+} doped LNCO cathodes. The structural and electrochemical characteristics of these cathode materials have been compared to establish that the Mo-doped cathodes (LNCMO) exhibit better electrochemical performance as compared to undoped LNCO cathodes.

2. Experimental

LNCO, LNCMO powders were synthesized by solid-state route using, Li_2O, NiO, Co_3O_4, MoO_3 as raw materials with >99.9% purity. Stoichiometric amount of the raw materials with 5 mole% excess Li_2O were weighed and ball-milled with propanol for 24 h. The resultant suspension was dried overnight in a laboratory oven, crushed using a mortar–pestle and calcined in the temperature range of 700–800 °C for 15–48 h for crystallization. The calcined powder was again crushed in a mortar–pestle to break agglomeration and sieved (using a 200 mesh) to yield the finer fraction of the calcined mass.

The phase formation behavior of the calcined powder was characterized by XRD using Cu Kα radiation in the 2θ ranges of 10–70°. Selected diffraction peaks were slow scanned at a scanning speed of 0.6° min^{-1}. From the recorded XRD pattern, the accurate peak position (2θ), integrated intensities, as well as the full-width at half maxima (FWHM) (β) of each slow scanned diffraction peaks was estimated by fitting them with Pearson VII amplitude function using a commercial peak fit software (Peakfit V4, Jandel Scientific). The Rietveld refinement was carried out using FullProf profile refinement program integrated with WINPLOTR for display and data analyses [7]. For structural refinement, a Pseudo Voigt peak shape was assumed and total 19 parameters (including the scale factor, five order background polynomial parameters, oxygen atomic positions, peak shape, asymmetry parameters, atomic occupancies, isotropic thermal parameters) were refined sequentially.

The electrochemical characteristics of the synthesized cathode powders were carried out in a two electrode test cell kept inside an argon filled glove box. A composite cathode was prepared as a mixture of the calcined oxide powder, carbon black, and poly-vinylidene fluoride (in the weight ratio of 80:10:10), emulsion with *n*-methyl-2-pyrrolidone in a slurry, painted on aluminum foil and vacuum dried overnight at 100 °C. Lithium metal foils were used as counter and reference electrode. 1 M $LiPF_6$, in a 1:1 (by weight) mixture of ethylene carbonate and dimethyl carbonate (DMC) was used as electrolyte. Celgard 2400 was used as separator between anode and cathode. A computer controlled potentiostat/galvanostat system [consists a PC 750.4 controller and PHE 200 software, Gamry Instruments] was used for charge–discharge measurements in a voltage range of 4.3–3.2 V at a constant current density of 0.45 mA cm^{-2} (~*C*/3).

3. Results and discussion

Fig. 1 shows the X-ray diffractograms of LNCO powder calcined at 800 °C for 15 h. Close inspection of the XRD pattern reveals the presence of impurity phase (marked as *). The impurity phase was indexed as Li_2CO_3 (JCPDS file #83-1454). Formation of this impurity phase has also been reported by others in $LiNiO_2$ as well as Co and Al co-doped $LiNiO_2$ cathode materials exposed in air for extended time [8,9]. Presumably, long time exposure of lithium nickel oxide based cathodes in air expedite the formation of this impurity phase and recently a surface reaction mechanism which involves the reaction among surface active oxygen (formed due to the reduction of Ni cations), atmospheric CO_2 and Li ion to form Li_2CO_3 impurity phase [8].

As shown in Fig. 1, higher intensity ratio of the (0 0 3) and (1 0 4) diffraction peaks as well as the clear splitting of the

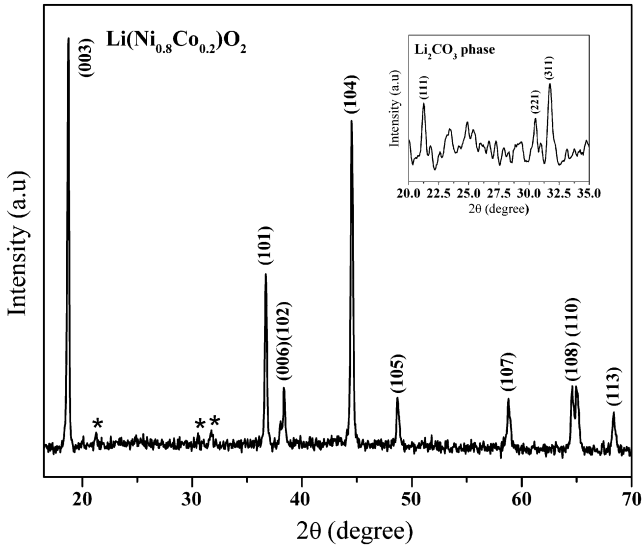

Fig. 1. X-ray diffractograms of $Li(Ni_{0.8}Co_{0.2})O_2$ powder calcined for 800 °C for 15 h. Inset shows the enlarged diffraction peaks for coexisted Li_2CO_3 impurity phase.

(0 0 6)/(1 0 2) and (1 0 8)/(1 1 0) diffraction peaks indicate excellent hexagonal layered structure of LNCO cathode [10–12]. The integrated intensity ratio of (0 0 3) and (1 0 4) peaks (I_{003}/I_{104}) have been considered as one of the indicators of the degree of cation mixing [13,14]. This is due to the fact that migration of Ni ions from the octahedral (3a) site to Li (3b) site (and vice versa) is reported to weaken the intensity of (0 0 3) line while such migrations do not alter the (1 0 4) peak intensity and as a result the ratio is decreased with increased cation mixing. Typically, in case of several hexagonal layered oxide cathodes reversible capacity has been reported to decrease when the ratio (I_{003}/I_{104}) is less than 1.2, for example, if the intensity ratio was observed to be below 1.0, $LiNiO_2$ has been reported to be electrochemically inactive [14]. Additionally, the *R factor* (defined by intensity ratio of $I_{006}/[I_{101}+I_{102}]$ is considered to be another indicator of the hexagonal ordering of the pristine cathode materials. Clear the splitting of the (0 0 6/1 0 2) peaks, better is the hexagonal ordering [15]. The X-ray diffraction peaks [(0 0 3) and (1 0 4), (1 0 1), (1 0 2) and (0 0 6)] were deconvoluted with Pearson VII amplitude function (using a commercial program Peakfit v4) (not shown). From the deconvoluted integrated intensities the parameters I_{003}/I_{104} and *R factor* were calculated to be 1.01 and 0.467, respectively. The calculated values indicate reasonably good hexagonal ordering in the pristine $Li(Ni_{0.8}Co_{0.2})O_2$ powders.

Fig. 2 shows the charge and discharge profiles of $Li(Ni_{0.8}Co_{0.2})O_2$ cathode after 2nd and 20th cycles in the cut-off voltage 4.3–3.2 V. As shown in the figure, the discharge capacity after the second cycle is ~100.0 mAh g^{-1} which drops down to ~72.40 mAh g^{-1} after 20th charge–discharge cycles (calculated retention ~63%). The lower capacity of the cathode material is thought to be related with the formation of Li_2CO_3 phase detected by XRD (Fig. 1). As detailed below the consequences of the impurity phase formation are as follows: in the first instance, the formation of this impurity phase could reduce the amount of lithium available for the intercalation and secondly,

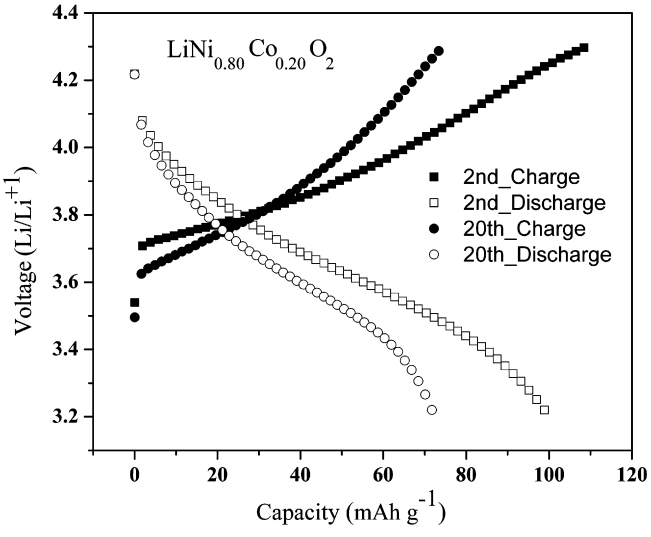

Fig. 2. Charge–discharge profiles of the $Li(Ni_{0.8}Co_{0.2})O_2$ cathode in a cut-off voltage range 4.3–3.2 V using 0.45 mA cm^{-2} current densities.

its presence also might increase the impedance of the cathode (since it has inferior electronic as well as ionic conductivities as compared to the active cathode material). The later would eventually affect adversely the discharge capacity as well as the cycleability as observed in the present case. Indeed, a discharge capacity as low as 25 mAh g^{-1} has been reported (discharged at *C*/6 rate) in the case of air exposed $LiNi_{0.8}Co_{0.15}Al_{0.05}O_2$ cathode as compared to the capacity ~65 mAh g^{-1} in case of freshly prepared cathode discharged at the same rate [9].

In case of sol–gel derived $Li(Ni_{0.8}Co_{0.2})O_2$, Liu et al. [16] has reported that the discharge capacity as well as the difference between the charge and discharge capacity after 1st cycle (polarization loss) has a strong correlation with the migration of Ni^{2+} (from 3a site) cation to the Li^{1+} (3b) site. Reduction of Ni^{3+} to Ni^{2+} and the migration of Ni^{2+} cations to the Li^{1+} site are dependent on the calcination time and temperature of the synthesized powder. During electrochemical charging (de intercalation) Ni^{2+} in 3b site is oxidized to Ni^{3+} and the resulting local structural disorder impede the subsequent Li^{1+} intercalation leading to capacity loss upon repeated charge–discharge cycling [17]. Viewing in this light, in the present work, in addition to the formation of the Li_2CO_3 impurity phase, calcination temperature and time as well as the partial pressure of oxygen during the heat treatment may also have their influence in deciding the final stoichiometry of the calcined powder and thereby the capacity of the composite cathode.

To gain insight about the structure–property relationship, using Fullprof program [7], we have performed the structural refinement (Rietveld analyses) of the XRD pattern of the pristine composite cathode. The following scheme was adopted to perform the Rietveld refinement. $LiNi_{0.8}Co_{0.2}O_2$ cathode assumed to crystallize in a hexagonal layered structure with $R\bar{3}M$ space group. Li_2CO_3, on the other hand crystallizes in a monoclinic structure having space group *C*2/*c* [18]. The atomic coordinates [for Li^{1+} (3b), Co^{3+}/Ni^{3+} (3a) and O^{2-} (6c) in $LiNi_{0.8}Co_{0.2}O_2$ and Li, C and O in Li_2CO_3] along with the preliminary lattice parameters of the respective phases are given in Table 1. In the first instance, all the atoms were assumed to occupy their respective positions as per the symmetry, whereas in the second instance, reduction of Ni^{3+} to Ni^{2+}, and cation mixing between Ni^{2+} in Li^{1+} (3b) and Li^{1+} in Ni^{3+}/Co^{3+} (3a) site was assumed and accordingly the atomic occupancy, lattice parameters, oxygen atomic positions (Z_{ox}) are refined. The assumed cation mixing model is justified as per as the neutron diffraction Rietveld refinement report of similar materials [19]. The above two refinement schemes are termed as without (no mixing) and with cation mixing (cation mixing) cases, respectively. The constraints of the structural refinement are as follows: each cation site was assumed to be fully occupied and the summation of the atomic fractions of the constituent atoms equals to one; number of cations equal to the number of anions and overall charge neutrality is maintained. The quality of the agreement between observed and calculated profiles is evaluated by profile factor (R_p), weighted profile factor (R_{wp}), expected weighted profile factor (R_{exp}), goodness of fit indicator (*S*), reduced chi-square (χ^2) and Bragg factor (R_B). The mathematical expressions of

Table 1
Atomic coordinates, space group and preliminary lattice parameters of $Li(Ni_{0.8}Co_{0.2})O_2$ and Li_2CO_3 impurity phase used in Rietveld structural refinement

Phase	Space group	Atom	Atomic coordinates			Lattice parameter (from JCPDS file)
$LiNi_{0.8}Co_{0.2}O_2$	$R\bar{3}M$ (hexagonal)	Li	0	0	0.5	$a=b=2.883$ Å; $c=14.19$ Å; $\alpha=\beta=90°$, $\gamma=120°$
		Ni/Co	0	0	0	
		O	0	0	0.25	
Li_2CO_3	$C2/c$ (monoclinic)	Li	0.1965	0.4484	0.8344	$a=8.361$ Å; $b=4.976$ Å; $c=6.93$ Å; $\alpha=\gamma=90°$, $\beta=114.69°$
		C	0	0.0657	0.25	
		O1	0	0.3213	0.25	
		O2	0.1459	0.3129	0.3127	

the above parameters are given below [7].

$$R_p = \frac{\sum_{i=1,n} |Y_i - Y_{c,i}|}{\sum_{i=1,n} Y_i} \times 100 \quad (1)$$

$$R_{wp} = \left[\frac{\sum_{i=1,n} w_i |Y_i - Y_{c,i}|^2}{\sum_{i=1,n} w_i Y_i^2} \right] \times 100 \quad (2)$$

$$R_{exp} = \left[\frac{n-p}{\sum_i w_i Y_i^2} \right] \times 100 \quad (3)$$

$$S = \frac{R_{wp}}{R_{exp}} \quad (4)$$

$$\chi^2 = \left[\frac{R_{wp}}{R_{exp}} \right]^2 \quad (5)$$

$$R_B = \frac{\sum_h |I_{i,h} - I_{c,h}|}{\sum_h |I_{i,h}|} \times 100 \quad (6)$$

The experimental (Y_i), calculated (Y_c) and the difference between experimental and calculated intensities ($Y_i - Y_c$) for *without* and with *cation mixing cases* for $Li(Ni_{0.80}Co_{0.20})O_2$ are shown in Fig. 3(a and b), respectively. The refined hexagonal cell parameters, Z_{ox}, isotropic thermal parameters, and fraction of Li_2CO_3 phase assuming with and without cation mixing is tabulated in Table 2. The reliability factors for XRD Rietveld refinement for the above cases and tabulated separately in Table 3. As shown in Table 3, both *cation mixing* as well as without *cation mixing* hypothesis lead equivalent reliability factors and therefore solely from the refined data it was not possible to favor one particular hypothesis over another. However, the presence of Li_2CO_3 impurity phase was detected unequivocally. In most of the published literature, Li_2CO_3 contents in lithium nickel oxide based cathodes have been determined using XRD phase analyses. The impurity phase fraction increases with the exposure time (in terms of several months to year) in open ambient. A wide scattering of Li_2CO_3 phase contents is reported, as for example, in $LiNi_{0.81}Co_{0.16}Al_{0.03}O_2$ cathode 8% Li_2CO_3 formation was estimated after 500 h exposure in ambient by Matsumoto et al. [20]. On the other hand, Li_2CO_3 contents in $Li_xNi_{0.8}Co_{0.15}Al_{0.05}O_2$ (LNCAO) cathode, freshly prepared and electrodes exposed for 2 years in air was reported to be 0.5 and 6.0 wt.%, respectively, by Zhuang et al. [9]. Liu et al. [8] estimated Li_2CO_3 content ~13.3 wt.% in $LiNiO_2$, exposed in air for 1 year. Usually Li_2CO_3 forms a continuous surface layer on active cathode particle [9] and this impurity layer has very detrimental effect on the discharge capacity. For example, at *C*/6 rate, the discharge capacity of fresh LNCAO (with 0.5 wt.% Li_2CO_3) drops down from 65 to 25 mAh g^{-1} in 2 years

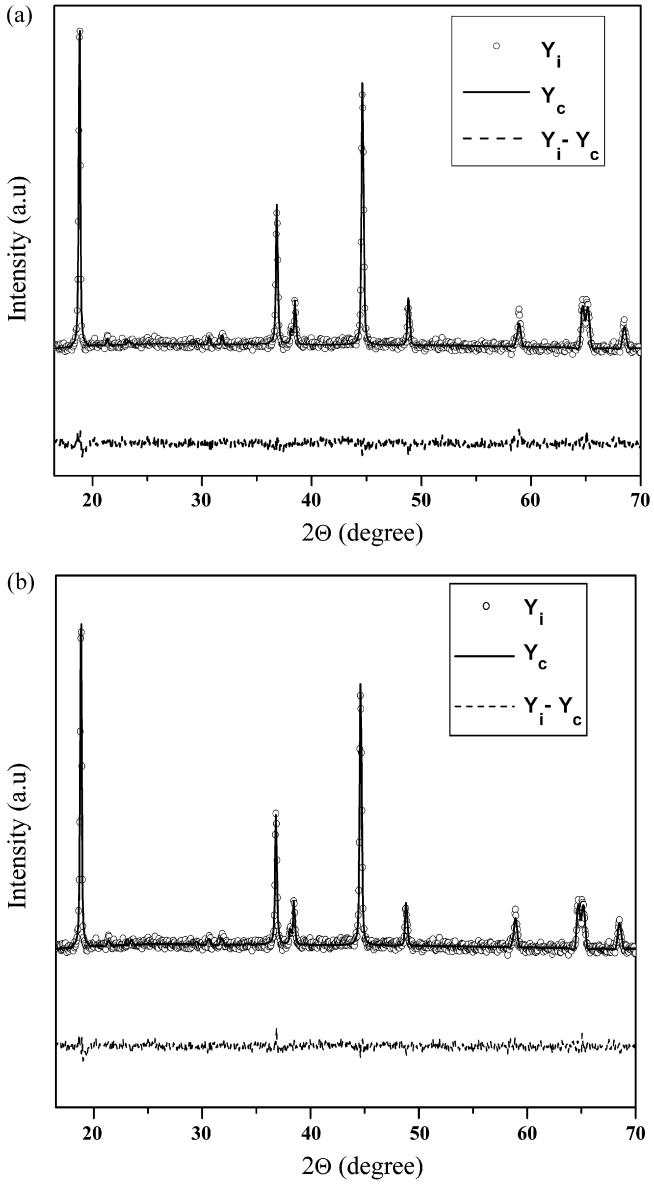

Fig. 3. Observed (Y_i), calculated (Y_c) and $Y_i - Y_c$ XRD patterns for $Li(Ni_{0.8}Co_{0.2})O_2$ cathode assuming: (a) without cation mixing and (b) cation mixing cases.

Table 2
Refined structural parameters and estimated fraction of $Li(Ni_{0.8}Co_{0.2})O_2$ and Li_2CO_3 impurity phase assuming without cation mixing as well as with cation mixing

$Li(Ni_{0.8}Co_{0.2})O_2$	a (Å)	b (Å)	c (Å)	Z_{ox}	B_{iso}	Li_2CO_3 (%)
Refined without cation mixing	2.862	2.862	14.154	0.2500	0.359	5.21
Refined with cation mixing	2.862	2.862	14.154	0.2500	0.359	5.39

Stoichiometry after refinement assuming without cation mixing $[Li_{1.0}{}^{1+}][Ni_{0.8}{}^{3+}Co_{0.2}{}^{3+}]O_2$ and with cation mixing $[Li_{0.975}{}^{1+}Ni_{0.025}{}^{2+}][Ni_{0.775}{}^{3+}Ni_{0.025}{}^{2+}Co_{0.2}{}^{3+}]O_2$.

Table 3
The estimated reliability factors for the $Li(Ni_{0.8}Co_{0.2})O_2$ structural refinement assuming without as well as with cation mixing cases

	R_p (%)	R_{wp} (%)	R_{exp} (%)	S	R_{Bragg} (%)	χ^2 (%)
$[Li_{1.0}{}^{1+}][Ni_{0.8}{}^{3+}Co_{0.2}{}^{3+}]O_2$	2.37	2.91	2.45	1.1877	12.5	1.41
$[Li_{0.975}{}^{1+}Ni_{0.025}{}^{2+}][Ni_{0.775}{}^{3+}Ni_{0.025}{}^{2+}Co_{0.2}{}^{3+}]O_2$	2.32	2.83	2.45	1.1532	11.8	1.33

air exposed electrode with 6% Li_2CO_3 contents. Similarly for air exposed $LiNiO_2$, with 13.3 wt.% Li_2CO_3 the cathode reported to be almost electrochemically inactive [8].

In the present work, two phase quantitative phase analysis was performed (using Rietveld refinement) and both for without and with cation mixing, the Li_2CO_3 contents in $Li(Ni,Co)O_2$ cathode was estimated to be ~5.2 wt.%. We have not studied the nature of distribution of the impurity phase in the synthesized cathode; however, from the above literature reports it is apparent that had the formed Li_2CO_3 remained as surface coated layer; the discharge capacity would have been drastically reduced. Considering this fact, we feel that in the present case Li_2CO_3 does not form a continuous surface layer on active LNCO cathode particles. Five mole percent excess Li_2O was added in making $LiNi_{0.8}Co_{0.2}O_2$ pristine cathode. It is probable that un-reacted Li_2O still remains after calcination which eventually reacts with atmosphere CO_2 to form Li_2CO_3 impurity phase. This phase separated, electrochemically inactive Li_2CO_3 reduces the discharge capacity not that drastically as it would do as coated layer with low ionic/electronic conductivity. More experiments are needed to be performed to clarify these issues.

Fp-Studio (v 1.0) [7] was used to visualize the layered structure from the refined structural parameters. Fig. 4 shows the schematic of the hexagonal layer structure of LNCO cathode. The Co/Ni–O slab (S) as well as Li position in the inter-slab spacing (I) are also marked in the figure. From the schematic it is clear that smaller the slab thickness (S), larger is the inter-slab spacing (I) which eventually leads to easier intercalation of the Li^+ ion during charge–discharge operation. The parameters S and I was calculated from the refined Z_{ox} and 'c' parameters using the following relations [19]

$$S_{(Co,Ni)O_2} = (\tfrac{2}{3} - 2Z_{ox})c \quad (7)$$

$$I_{(LiO_2)} = \tfrac{c}{3} - S_{(Co,Ni)O_2} \quad (8)$$

A separate program Bond_Str was used to calculate the cation–cation, cation–anion and anion–anion bond lengths from the refined structural parameters. The results of these calculations are tabulated in Table 4. The calculated parameter compares well with the similar parameters reported in case of $LiNi_{0.8}Co_{0.2}O_2$ cathode prepared by sol–gel technique [16].

As mentioned earlier, the lower discharge capacity of the $LiNi_{0.8}Co_{0.2}O_2$ cathode in the present case could be related to the existence of electrochemically inactive Li_2CO_3 phase. Additionally, the discharge capacity of the synthesized cathode depends on the calcination temperature–time combination as well as on the discharge current (C rate). For example, at C/10 discharge rate H. Liu et al. [16] reported the discharge capacity in the range of 131–180 mAh g^{-1} when the calcination temperature time combinations were in the range of 998–1073 K for 12–36 h. For pristine $LiNi_{0.8}Co_{0.15}Al_{0.05}O_2$ cathode Zhuang et al. [9] reported that the discharge capacity reduces from 130 to 50 mAh g^{-1} when rate current was progressively changed from

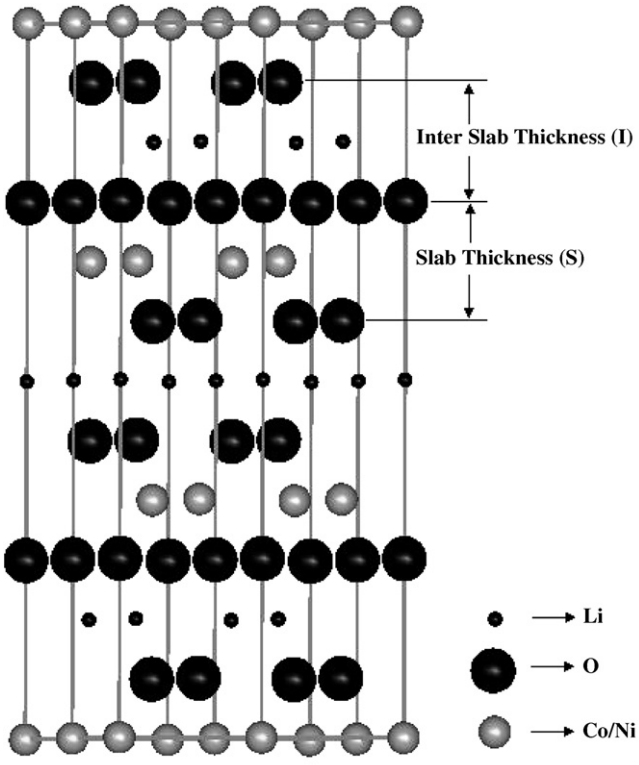

Fig. 4. Schematic of the hexagonal layer structure of $Li(Ni_{0.8}Co_{0.2})O_2$ derived from the Rietveld refinement. The $(Co,Ni)O_2$ slab (S) as well as the LiO_2 layer in the inter-slab spacing (I) is also marked in the diagram.

Table 4
Estimated cation–cation, cation–anion, and anion–anion bond lengths, slab thickness (S) and inter-slab spacing (I) of schematic of pristine $Li(Ni_{0.8}Co_{0.2})O_2$ cathode

	Li–Li (Å)	Li–Ni/Co (Å)	Li–O (Å)	O–O (Å)	O–O′ (Å)	S (Å)	I (Å)
$[Li_{1.0}^{1+}][Ni_{0.8}^{3+}Co_{0.2}^{3+}]O_2$	2.862	2.880	2.030	2.862	2.880	2.359	2.359
$[Li_{0.975}^{1+}Ni_{0.025}^{2+}][Ni_{0.775}^{3+}Ni_{0.025}^{2+}Co_{0.2}^{3+}]O_2$	2.862	2.880	2.064	2.862	2.974	2.359	2.359

$C/44$ to $C/2$. In the present case we have used discharge rate $\sim C/3$ which yield discharge capacity $\sim$100 mAh g^{-1}. Even if the cation disorder in LNCO has its effect on the lowered capacity as well as observed capacity fading, simply by performing XRD Rietveld refinement this cannot be established unequivocally. Additional supportive experimental proof is necessary to gain further insight about the observed electrochemical properties.

To improve the performance of the $Li(Ni_{0.8}Co_{0.2})O_2$ (LNCO) cathode, it is imperative to avoid the formation of Li_2CO_3 impurity phase. In addition to that, for better intercalation of Li^+ during charge–discharge, the inter-slab spacing (I) should be increased. Cation doping into the host LNCO structure is considered to be an effective way to improve the electrochemical characteristics of the pristine LNCO cathode. Accordingly, part of Co^{3+} in the host LNCO lattice is substituted with Mo^{6+} to prepare $Li(Ni_{0.8}Co_{0.15}Mo_{0.05})O_2$ (LNCMO) cathode. Since the ionic radii of Co^{3+} and Mo^{6+} ions are similar [0.61 and 0.59 Å, respectively (CN = 6)], Mo substitution is structurally favorable. In addition to that the smaller ionic radius of Mo^{6+} is expected to reduce the $(Ni,Co,Mo)O_2$ octahedral slab thickness (S) and thereby increase the inter-slab spacing (I) for easier intercalation of Li^+ ions during electrochemical charge–discharge cycling. Easier intercalation in turn is expected to improve the electrochemical properties of LNCMO cathodes.

XRD pattern of LNCMO powders annealed at 800 °C for 24 h yield hexagonal order structure without the formation of any Li_2CO_3 impurity phase. Fig. 5 shows the charge–discharge behavior of LNCMO cathode after 2nd and 20th cycles in a cut-off voltage range of 4.3–3.2 V. As shown in the figure, the discharge capacity after the second cycle is $\sim$157 mAh g^{-1} which drops down to $\sim$140 mAh g^{-1} after 20th charge–discharge cycles (retention $\sim$89%). Comparing Figs. 2 and 5, it is apparent that in Mo modified LNCO cathodes; both the discharge capacity ($\sim$157 mAh g^{-1} in comparison to $\sim$100 mAh g^{-1}) and capacity retention (89% in comparison to 63%) has significantly been improved. In summary, our experimental results show that LNCMO cathode is phase pure (free from Li_2CO_3 phase) and Mo as a dopant improves the discharge capacity as well as cycleability in these cathodes.

In order to gain insight on the improvement of the Mo modified LNCO cathode, we have performed the structural refinement

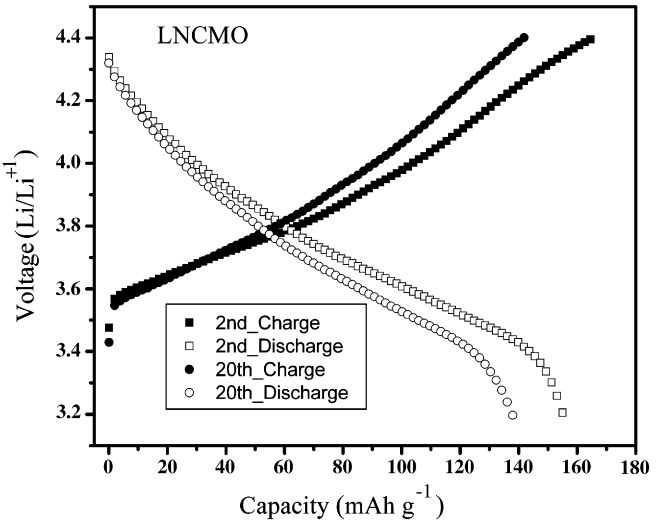

Fig. 5. Charge–discharge profiles of the LNCMO cathode in a cut-off voltage range 4.3–3.2 V using 0.45 mA cm^{-2} current densities.

of the XRD pattern of the LNCMO composite cathode. The experimental (Y_i), calculated (Y_c) and ($Y_i - Y_c$) intensities for without and with cation mixing cases for LNCMO cathodes are shown in Fig. 6(a and b), respectively. In Fig. 6(a) we have assumed Mo^{6+} ions in the cobalt site whereas in Fig. 6(b) part of the Mo^{6+} ion has been assumed to occupy the Li^+ site and part of Li^+ ion is assumed to occupy the Ni^{3+}/Co^{3+} site. For both these cases, the refined structure parameters as well as the reliability factors are tabulated in Tables 5 and 6. As shown in the refined patterns as well as Table 5, Rietveld refinement, in both the assumed cases yield similar results which render it difficult to support one particular hypothesis over the other. However, comparing Tables 2 and 5, we could find that Mo doped LNCO cathode has slightly reduced 'a' parameter (2.859 Å as compared to 2.862 Å in undoped LNCO) and Z_{ox} is increased to 0.2559 (as compared to 0.2500 in LNCO cathode). The refined 'c' parameter of Mo doped composition is slightly decreased as compared to its undoped counterpart. Table 7 compares the cation–cation, cation–anion, anion–anion bond lengths, along with the slab thickness (S) and inter-slab spacing (I) for without and with cation mixing cases of LNCMO composite cathodes.

Table 5
Refined structural parameters of LNCMO assuming without cation mixing as well as with cation mixing

Mo doped LNCO	a (Å)	b (Å)	c (Å)	Z_{ox}	B_{iso}
Refined without cation mixing	2.859	2.859	14.151	0.2559	0.728
Refined with cation mixing	2.859	2.859	14.153	0.2559	2.641

Stoichiometry after refinement assuming without cation mixing $[Li_{1.0}^{1+}][Ni_{0.65}^{3+}Ni_{0.15}^{2+}Co_{0.15}^{3+}Mo_{0.05}^{6+}]O_2$, and with cation mixing $[Li_{0.975}^{1+}Mo_{0.025}^{6+}][Ni_{0.65}^{3+}Ni_{0.15}^{2+}Co_{0.15}^{3+}Mo_{0.025}^{6+}Li_{0.025}^{1+}]O_2$.

Table 6
The estimated reliability factors for the LNCMO structural refinement assuming without mixing as well as with cation mixing

	R_p (%)	R_{wp} (%)	R_{exp} (%)	S	R_{Bragg} (%)	χ^2 (%)
$[Li_{1.0}^{1+}][Ni_{0.65}^{3+}Ni_{0.15}^{2+}Co_{0.15}^{3+}Mo_{0.05}^{6+}]O_2$	3.04	3.92	9.19	0.4265	1.40	0.182
$[Li_{0.975}^{1+}Mo_{0.025}^{6+}][Ni_{0.65}^{3+}Ni_{0.15}^{2+}Co_{0.15}^{3+}Mo_{0.025}^{6+}Li_{0.025}^{1+}]O_2$	3.05	3.94	9.19	0.4289	2.86	0.184

Table 7
Estimated cation–cation, cation–anion, and anion–anion bond lengths, slab thickness (S) and inter-slab spacing (I) of schematic of pristine LNCMO cathode

Material	Li–Li (Å)	Li–Ni/Co (Å)	Li–O (Å)	O–O (Å)	O–O′ (Å)	S (Å)	I (Å)
$[Li_{1.0}^{1+}][Ni_{0.65}^{3+}Ni_{0.15}^{2+}Co_{0.15}^{3+}Mo_{0.05}^{6+}]O_2$	2.858	2.879	2.087	2.8588	3.041	2.1913	2.5258
$[Li_{0.975}^{1+}Mo_{0.025}^{6+}][Ni_{0.65}^{3+}Ni_{0.15}^{2+}Co_{0.15}^{3+}Mo_{0.025}^{6+}Li_{0.025}^{1+}]O_2$	2.858	2.879	2.079	2.8589	3.020	2.1916	2.5262

By comparing Table 7 with Table 4, it is observed that in case of without cation mixing Li–O as well as O–O′ bond lengths are significantly increased (O and O′ are the two out of the plane oxygen atoms in the oxygen octahedral). The calculated slab thickness (S) is reduced and the inter-slab spacing (I) is increased in LNCMO composite cathode.

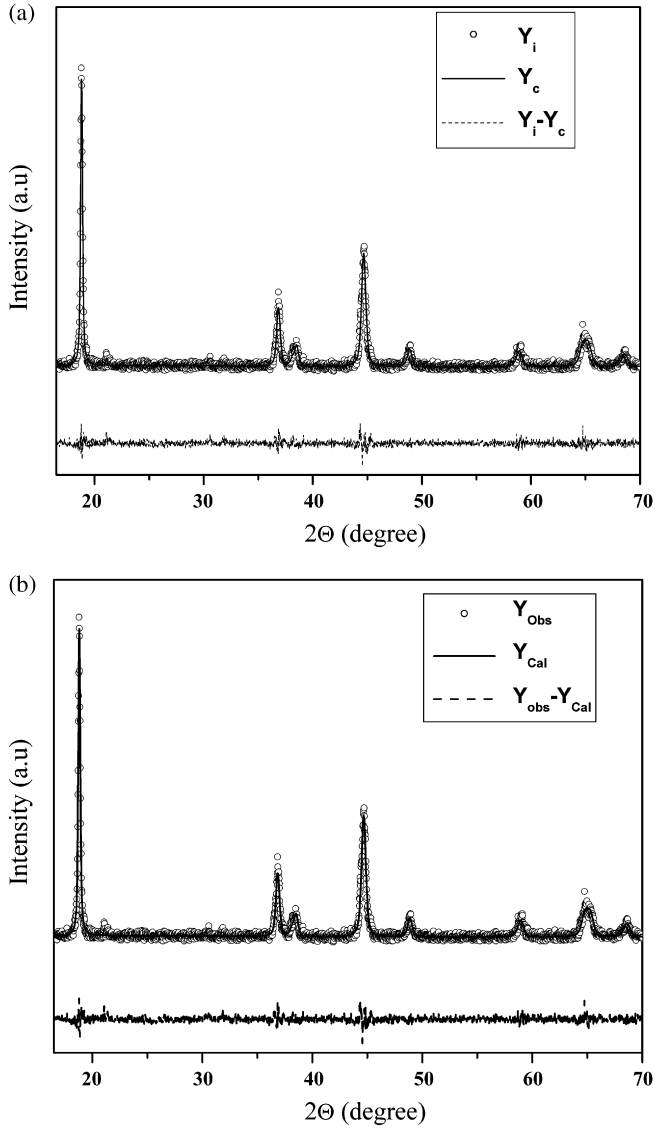

Fig. 6. Observed (Y_i), calculated (Y_c) and $Y_i - Y_c$ XRD patterns for LNCMO cathode assuming: (a) without cation mixing and (b) cation mixing cases.

Although the cation disorder, i.e. the migration of Ni/Co ions in Li layers (and vice versa) has been reported in the literature [16,21], as observed in the present work, merely from Rietveld refinement, any such cation disorder could not be established unequivocally both in LNCO as well as LNCMO pristine cathode materials. Similar conclusion has also been made by Guilmard et al. [19] in case of $Li(Ni_{0.90}Mn_{0.10})O_2$ cathode material. In their case even after neutron diffraction pattern refinement any particular cation mixing hypothesis could not be established. However, from our refinement analyses it is clear that Mo as a dopant increases the $(Ni,Co)O_2$ inter-slab thickness providing easier Li^+ movement which in turn increases the discharge capacity of LNCMO cathode as compared to the undoped LNCO cathode. Additionally, in Mo doped LNCO cathode, no impurity phase (such as Li_2CO_3) was detected. The phase pure LNCMO cathode yields increased discharge capacity as compared to its undoped counterpart. The inclusion of Mo^{6+} ions in the LNCO lattice is indicated both from the reduction of 'a' parameter as well as change in calculated bond lengths as shown in Table 6. In layered cathode materials (e.g. $LiCoO_2$), doped with electrochemically inactive dopant cations (e.g. Mg^{2+} or Zr^{4+}) it has been hypothesized [22] that the dopants move to the $(Co,M)O_2$–$(Co,M)O_2$ inter-slab position during the Li^{1+} de-intercalation and act as a pillar which in turn assist the movement of Li^+ ion by preventing the lithium vacancy ordering and hindering the migration of the cations from the $(Ni,Co)O_2$ slab to the lithium site [23]. Probably similar mechanism is also operative in the present case and due to the so called "pillaring effect" of the Mo dopant, easier Li^{1+} intercalation is maintained upon repeated charge–discharge cycling which in turn increases the cyleability of the LNCMO cathode as compared to its undoped (LNCO) counterpart. Further research is required to clarify these issues.

4. Conclusions

In the present work conventional solid-state reaction route was adopted to prepare LNCO and Mo modified LNCO (LNCMO) cathode materials for lithium ion rechargeable batteries. In the cut-off voltage range 4.3–3.2 V using a current density of 0.45 mA cm^{-2}, the discharge capacity of the LNCO

was found to be 100.05 mAh g^{-1}, with a capacity retention of ∼63% after 20 charge discharge cycles. Both the initial discharge capacity (∼157 mAh g^{-1}) as well as capacity retention (∼89%) after 20th charge–discharge cycles is significantly increased in LNCMO cathodes. Rietveld analyses of the high-resolution X-ray diffraction patterns of the pristine composite cathodes have been performed to gain insight on the observed behavior. The relatively lower discharge capacity of the undoped LNCO cathode is thought to be related with the formation of Li_2CO_3 impurity phase. The mechanism of the formation of the Li_2CO_3 impurity phase in the freshly prepared pristine LNCO cathode is not clearly understood. Further research is required to discern the nature of the distribution of the impurity phase in them. In the LNCMO cathode no such impurity phase was detected. From XRD Rietveld analyses of the Mo modified cathode, the lattice parameter as well as oxygen atomic positions were determined and using these parameters the $(Co,Ni)O_2$ slab thickness and inter-slab spacing were estimated. Mo doping was found to increase the $(Co,Ni)O_2$ inter-slab spacing which imparts easier Li^+ ion intercalation. Both these factors have been argued to be responsible for the significant increment of the discharge capacity of the LNCMO cathode. Probably, Mo as a dopant, during repeated charge–discharge cycle too, maintain easier Li^+ ion intercalation which results in improved cycleability as compared to its undoped counterpart.

Acknowledgments

The above research work was partially supported by the research grants from DoE (# DE-FG02-01ER45868) and NASA (#NAG3-2676) Glenn Research Center. The high-resolution XRD measurements were carried out utilizing the facilities at the Central Research Facilities (CRF) at the Indian Institute of Technology, Kharagpur, India.

References

[1] C. Delmas, L. Croguennec, Mater. Res. Soc. Bull. (2002) 608.
[2] I. Nakai, T. Nakagome, Electrochem. Soild. State. Lett. 1 (1998) 259.
[3] H. Omanda, T. Brousse, C. Marhic, D.M. Schleich, J. Electrochem. Soc. 151 (2004) A922.
[4] A.M. Kannan, A. Manthiram, J. Electrochem. Soc. 150 (2003) A349.
[5] S. Choi, A. Manthiram, J. Electrochem. Soc. 149 (2002) A1157.
[6] T. Ohzuku, T. Yanagawa, M. Kouguchi, A. Ueda, J. Power Sources 68 (1997) 131.
[7] H.M. Rietveld, J. Appl. Crystallogr. 2 (1969) 65, Fullprof. Suite program available at http://www.llb.cea.fr/fullweb/fp2k/fp2k.htm.
[8] H.S. Liu, Z.R. Zhang, Z.L. Gong, Y. Yang, Electrochem. Solid State Lett. 7 (2004) A190.
[9] G.V. Zhuang, G. Chen, J. Shim, X. Song, P.N. Ross, T.J. Richardson, J. Power Sources 134 (2004) 293.
[10] S.B. Majumder, S. Nieto, R.S. Katiyar, J. Power Sources 154 (2006) 262.
[11] P. Periasamy, H.S. Kim, S.H. Na, S.I. Moon, J.C. Lee, J. Power Sources 132 (2004) 213.
[12] B.J. Hwang, R. Santhanam, C.H. Chen, J. Power Sources 114 (2003) 244.
[13] D. Li, Y. Sasaki, K. Kobayakawa, Y. Sato, J. Power Sources 157 (2006) 488.
[14] T. Ohzuku, A. Ueda, M. Nagayama, Y. Iwakoshi, H. Komori, Electrochim. Acta 38 (1993) 1159.
[15] Y. Gao, M.V. Yakovleva, W.B. Ebner, Electrochem. Solid State Lett. 1 (1998) 117.
[16] H. Liu, Jie Li, Z. Zhang, Z. Gong, Y. Yang, J. Solid State Electrochem. 7 (2003) 456.
[17] C. Delmas, M. Menetrier, L. Croguennec, I. Saadoune, A. Rougier, C. Pouillerie, G. Prado, M. Grune, I. Fournes, Electrochim. Acta 45 (1999) 243.
[18] H. Effenberger, J. Zemann, Z. Kristallogr. 150 (1979) 133.
[19] M. Guilmard, L. Croguennec, C. Delmas, J. Electrochem. Soc. 150 (2003) A1287.
[20] K. Matsumoto, R. Kuzuo, K. Takeya, A. Yamanka, J. Power Sources 81/82 (1999) 558.
[21] T. Gross, T. Buhrmester, K.G. Bramnik, N.N. Bramnik, K. Nikolowski, C. Baehtz, H. Ehrenberg, H. Fuess, Solid State Ionics 176 (2005) 1193.
[22] H.S. Kim, T.K. Ko, B.K. Na, W.I. Cho, B.W. Chao, J. Power Sources 138 (2004) 232.
[23] C. Pouillerie, L. Crohuennec, P. Biensan, P. Willmann, C. Delmas, J. Electrochem. Soc. 147 (2000) 2061.